C. R. Mecanique 340 (2012) 501–511

Contents lists available at SciVerse ScienceDirect

Comptes Rendus Mecanique

www.sciencedirect.com

Analytical and innovative solutions for heat transfer problems involving phase change and interfaces

On the boundary immobilization and variable space grid methods for transient heat conduction problems with phase change: Discussion and refinement

Méthodes d'immobilisation de l'interface et du pas d'espace variable appliquées au problème de conduction instationnaire de la chaleur avec changement de phase : Discussion et amélioration

Nacer Sadoun [a,b,*], El-Khider Si-Ahmed [a,c], Pierre Colinet [b], Jack Legrand [c]

[a] *Laboratoire de mécanique des fluides théorique et appliquée, faculté de physique, université des sciences et de la technologie Houari Boumediene (USTHB), BP 32, El-Alia, 16111 Alger, Algeria*

[b] *Service transferts, interfaces et procédés (TIPs), faculté des sciences appliquées/École polytechnique, université libre de Bruxelles (ULB), CP165/67, 50, avenue F.D. Roosevelt, B-1050 Bruxelles, Belgium*

[c] *LUNAM université, université de Nantes, CNRS, GEPEA UMR-6144, BP 406, 37, boulevard de l'Université, 44602 Saint-Nazaire cedex, France*

ARTICLE INFO

Article history:
Available online 15 May 2012

Keywords:
Stefan problem
Numerical solution
Finite differences
Variable space grid
Boundary immobilization
Accuracy refinement

Mots-clés :
Problème de Stefan
Solution numérique
Différences finies
Maillage spatial variable
Immobilisation de frontière
Amélioration de la précision

ABSTRACT

Explicit numerical schemes obtained using variable space grid (VSGM) and boundary immobilization (BIM) methods are considered for the solution of the transient heat conduction problem with phase change. This article briefly reviews different approaches developed to track the phase change front with a particular interest to those tracking explicitly the moving boundary. The analysis shows that both methods lead to identical computational algorithm, then considers the modified numerical scheme developed by Kutluay et al. (J. Comput. Appl. Math. 81 (1997) 135–144) and proposes a refinement procedure for the scheme without any additional CPU time. Two Stefan-like problems, having exact solutions, are studied and numerical results are assessed with respect to their performances.

© 2012 Académie des sciences. Published by Elsevier Masson SAS. All rights reserved.

RÉSUMÉ

Les schémas numériques obtenus à partir des méthodes fixant la frontière mobile (BIM) ou adaptant le pas de discrétisation spatiale au mouvement de celle-ci (VSGM) sont appliqués au problème de conduction instationnaire avec changement de phase. L'article revoit brièvement les différentes approches développées pour le suivi d'interface avec une attention particulière pour celles la localisant explicitement. L'analyse, qui montre que les deux schémas ne sont que deux expressions différentes d'une même solution, porte également sur la modification apportée par Kutluay et al. (J. Comput. Appl. Math. 81 (1997) 135–144) et propose une procédure sure pour améliorer la précision de la solution.

* Corresponding author at: Service transferts, interfaces et procédés (TIPs), faculté des sciences appliquées/École polytechnique, université libre de Bruxelles (ULB), CP165/67, 50, avenue F.D. Roosevelt, B-1050 Bruxelles, Belgium.

E-mail addresses: nsadoun@ulb.ac.be (N. Sadoun), esi-ahmed@usthb.dz (E.K. Si-Ahmed), pcolinet@ulb.ac.be (P. Colinet), Jack.Legrand@univ-nantes.fr (J. Legrand).

1631-0721/$ – see front matter © 2012 Académie des sciences. Published by Elsevier Masson SAS. All rights reserved.
doi:10.1016/j.crme.2012.03.003

L'application de ces schémas numériques à deux exemples de problème de Stefan permet de comparer leurs performances.

© 2012 Académie des sciences. Published by Elsevier Masson SAS. All rights reserved.

1. Introduction

The transient heat conduction problem involving phase change is of increasing interest in many todays applications including, among others, renewable energy using latent heat storage system, welding and casting technology, crystal growth of semiconductors and metals, food processing industry, etc. The solution of such problems is inherently difficult because of the nonlinear form of the thermal energy balance equation at the unknown variable solid/liquid interface. The latter, being part of the solution, has a priori to be located and followed. Closed analytical solutions are difficult to obtain except for problems which must be adaptable to similarity transformations [1] or governed by fractional diffusion equation which employs space and time fractional derivatives [2,3]. Then, recourse is made to approximate techniques to solve the problem. As a result, various experimental, numerical and approximate analytical methods, subject of many comprehensive books and papers [4–12], are developed successfully and applied to various problems.

The analytical approaches encompass the use of perturbation technique [13,14], heat balance integral [15–18], refined integral [19–22], integral iterative formulation [23,24], integral with fractional diffusion [2,3,25], power series expansion [6], similarity [26] and even electrical analogy techniques [27].

On the other hand, the numerous and various numerical methods developed can be conveniently handled into explicit or implicit methods according to the moving boundary location procedure. This classification, as discussed at a later stage, differs from that suggested by Gupta [4] or Crank [5], particularly with respect to the explicit methods.

In the implicit methods, the solution of the energy equation does not require knowledge of the solid/liquid interface position which is implicitly deduced from the enthalpy or temperature distribution [28]. The methods also referred to as "one-phase methods" or "enthalpy methods" treat the domain solid/liquid as one phase with strong temperature dependence of thermophysical properties. The heat balance equation at the interface is implicitly included in a new form of the energy equation valid for the whole domain. The reader can refer to the review papers of Voller et al. [29] for the implicit methods dealing with the pure conduction and of Samarski et al. [30] which takes into account the conduction/convection coupling.

In the explicit methods, the phasic governing equations are to be considered and coupled at the interface by the temperature and the energy balance. The location of the moving front, tracked at each time step, constitutes a part of the problem solution making then the latter more complex due to the nonlinear form of the energy balance equation at the interface. The methods are also referred to as "two-phase methods" or "front-tracking methods" and can be categorized into "front-moving method" and "front-fixing method".

The front-moving method was introduced by Crank [31], subsequently refined by Murray and Landis [32] and more recently by Verma et al. [33]. The space–time domain discretization within the moving front (liquid/solid) is based on a fixed mesh. Using the interpolation formulas in the neighborhood of the phase change zone, equations are established to track, in between nodes, the moving front. However, the irregularity of the mesh in the vicinity of the interface is the source of numerical instabilities and the implementation complexity of the resulting numerical schemes.

The front-fixing methods are the techniques which have received more attention. They always locate the moving interface on a given grid point by adapting either the time integration step or the space step according to the front movement. Variable time space methods consist on fixing the space step and to adapt, at each integration, the time step so that the front travels the distance between two consecutive nodes. Hence, even if the space domain subdivision can be kept regular, a predictor–corrector iteration process is required [34–36]. Similarly, the variable space grid approach sets the last grid point at the moving interface after determining its position using the conditions at this boundary [32,37–42]. The space width interval changes according to the movement of the interface. Two additional approaches locate the moving front on a given mesh point using a variable transform. The first, known as the boundary immobilization method [31,38,40,41], introduces the Landau variable to fix the computational space domain to $[0, 1]$ and locates the moving front at the boundary-end. The space–time domain is subdivided into a rectangular grid system with constant space and time increments. The second, called the isothermal migration method, permutes the dependent and independent variables and proceeds by tracking the trajectory of isotherms rather than determining the temperature distribution. The spatial position becomes the dependent variable of time and temperature and the moving front is tracked through the trace of the phase change isotherm. The technique was introduced by Dix and Cizek [43] and Chernousko [44] and developed later by Crank and Ozis [45], Wood [46] and more recently by Kutluay and Esen [47]. This technique, less accurate with a restrictive domain of application, considers a boundary-fixing method.

The present work concerns application of two numerical explicit methods based on front-tracking technique, called respectively variable space grid (VSGM) [32] and boundary immobilization (BIM) [31] methods. Their main advantage is a considerable simplified numerical effort. Two Stefan-like problems are taken as physical models. Both of them concern the one-phase Stefan problem: one deals with a heat source or sink [48] whereas the second concerns an exponentially increasing heat flux at the boundary [49]. It is worth noticing that the solution of both problems are considered numerically in Refs. [40] and [38] respectively.

The contribution of the article aims at showing that the numerical schemes obtained by the above cited methods lead to the same computational algorithm. Then, for given initial boundary conditions, time stepping and space grid, both methods lead to the same solution. Furthermore, it considers the modified boundary immobilization scheme used by Kutluay et al. [38] and demonstrates that it is less accurate than the usual scheme and a way to refine the accuracy of the latter's is proposed.

2. Problem statement

Consider the freezing of a semi-infinite liquid initially at its melting temperature $U(x,t)=0$. The liquid, in the region $x \geqslant s_0$, is in contact with a finite solid of the same material, initially at temperature $U(x,0)=g(x)$. Solidification is instantaneously initiated due to the outgoing heat flux at the boundary. By noting, s and v, respectively, the position and the velocity of freezing front at time t, and assuming a forcing term (sink of heat) $f(x,t)$ acting on the solid region $0 \leqslant x \leqslant s(t)$, the temperature distribution $U(x,t)$ is governed by the following heat conduction equation in the solidified layer

$$\frac{\partial U(x,t)}{\partial t} = \frac{\partial^2 U(x,t)}{\partial x^2} + f(x,t), \quad 0 < x < s(t),\ t > 0 \tag{1}$$

with a uniform temperature beyond the freezing point that is:

$$U(x,t) = 0, \quad x > s(t),\ t > 0 \tag{2}$$

In most moving boundary problems, two conditions are available at the interface, $x = s(t)$. In this case, the first provides one of the two boundary conditions required for the integration of Eq. (1), while the second locates the interface itself through a relationship defining the front velocity, $v(t)$. Both conditions read, respectively as

$$U(x,t) = 0, \quad x = s(t),\ t > 0 \tag{3}$$

$$v(t) = \frac{\mathrm{d}s}{\mathrm{d}t} = -\frac{\partial U(x,t)}{\partial x}, \quad x = s(t),\ t > 0 \tag{4}$$

and refer to the phase change temperature (Eq. (3)) and the well-known Stefan condition (Eq. (4)). The latter is derived from the heat balance requirement at the moving boundary with initial condition, specified by the initial thickness of the solidified layer, that is:

$$s(t) = s_0, \quad t = 0 \tag{5}$$

In addition to the boundary condition (Eq. (3)), two relations are required for the solution of the second-order partial differential equation (1). The first expresses the initial temperature distribution as follows:

$$U(x,t) = g(x), \quad 0 \leqslant x \leqslant s_0,\ t = 0 \tag{6}$$

The second, closing the mathematical model, is given on the fixed boundary $x = 0$ and depends on the problem considered. We denote by *FBC* (Fixed Boundary Condition) this closure; that is:

$$FBC, \quad x = 0 \tag{7}$$

The two problems examined numerically, using both VSGM and BIM, by Kutluay [40] and Kutluay et al. [38] are expressed hereafter.

2.1. Problem 1: Stefan problem with forcing term

This problem considers one-phase Stefan problem with a forcing term and imposed zero temperature at the boundaries $x = 0$ and $x = s(t)$. The solidification process initiation is due to the initial temperature distribution in the solid region leading mathematically to the following:

$$s_0 = 1, \quad t = 0 \tag{8}$$

$$f(x,t) = xe^t + 2, \quad 0 \leqslant x \leqslant s(t),\ t \geqslant 0 \tag{9}$$

$$g(x) = x(1-x), \quad 0 \leqslant x \leqslant s_0,\ t = 0 \tag{10}$$

$$U(0,t) = 0, \quad t \geqslant 0 \tag{11}$$

The mathematical model described by Eqs. (1)–(6), (8)–(11) admits an exact analytical solution for the temperature distribution and the freezing front location. The solution, demonstrated by Fasano and Primicerio [48], was recently obtained by applying the heat balance integral method [16], as follows:

$$U(x,t) = x\left(e^t - x\right), \quad 0 \leqslant x \leqslant s(t),\ t \geqslant 0 \tag{12}$$

$$s(t) = e^t, \quad t \geqslant 0 \tag{13}$$

2.2. Problem 2: Stefan problem with time-dependent heat flux at the boundary

The classical one-phase Stefan problem (no forcing term) with time-dependent heat flux, instead of a fixed temperature, at the boundary $x = 0$ is considered. The half space $x \geqslant 0$ is entirely liquid and subjected to an exponential time-decreasing heat flux at its boundary. Mathematically, that is expressed by the following equations

$$s_0 = 0 \tag{14}$$

$$f(x,t) = 0, \quad x \geqslant 0,\ t \geqslant 0 \tag{15}$$

$$g(x) = 0, \quad x \geqslant 0,\ t = 0 \tag{16}$$

$$\frac{\partial U}{\partial x} = -e^t, \quad x = 0,\ t \geqslant 0 \tag{17}$$

The following exact solution, as given by Hoffmann [49], holds:

$$U(x,t) = e^{t-x} - 1, \quad 0 \leqslant x \leqslant s(t),\ 0 < t < 1 \tag{18}$$

$$s(t) = t \tag{19}$$

It is worth stressing that the above exact solutions are obtained in order to satisfy specific mathematical requirements. The boundary conditions are chosen in a way that the ordinary differential equations resulting from the analysis present exact analytical solutions. Unfortunately, the obtained solutions and the corresponding problems did not concern any physical or industrial situation. As an example, the solution of Problem 2 is obtained imposing constant phase change rate which, to our knowledge, is irrelevant to any application.

3. Numerical solutions

Various numerical schemes can be used to solve the above governing equations [4,5], with a particular interest to those using the variable space grid and boundary immobilization techniques developed respectively by Murray and Landis [32] and Crank [31]. Both methods, reformulate the mathematical model to locate the liquid/solid interface, at given grid point, which is moving in the first method and fixed in the second. The transformed heat transfer equations will be solved using explicit finite differences approximations. The temporal derivatives, in the resulting transport equations and boundary conditions, are replaced by partial discretization based on forward difference approximations. On the other hand, the spatial derivative is approached using central differences in transport equations and backward or forward differences in the boundary conditions. Thus, the local truncation error order is proportional to the sum of the time step and the square of the space step sizes.

In both methods, the time interval Δt is kept constant and the space domain is divided into N intervals of equal width having the first grid point $(i = 1)$ lying on the fixed boundary while the last one $(i = N + 1)$ is located on the moving boundary. We denote by s^j, v^j and U_i^j respectively the position, the velocity of the moving boundary and the temperature of the ith grid point at time $t^j = j\Delta t$ $(j = 1, 2, \ldots)$.

3.1. Variable space grid method (VSGM)

In the VSGM, the moving boundary is always fixed at the last grid point by increasing the space width interval as the solidified layer grows. The domain is divided into N intervals each having a width of $(1/N)$ times the depth of the region of interest. If we denote Δx^j its size at time t^j $(j = 1, 2, \ldots)$, then any point (x_i, t_j) in the x–t domain is given by $((i-1)\Delta x^j, j\Delta t)$. Before working over the discretization, the mathematical model is written over according to Murray and Landis's [32] formulation. The model examines the partial derivation with respect to time by tracking a given line instead of at constant x. For the line located at the ith grid point, the conduction equation reads:

$$\left.\frac{\partial U}{\partial t}\right)_{x_i} = v(t)\frac{x_i}{s}\left.\frac{\partial U}{\partial x}\right)_t + \left.\frac{\partial^2 U}{\partial x^2}\right)_t + f(x_i,t), \quad 0 \prec x \prec s(t),\ t \succ 0 \tag{20}$$

Suffices x and t mean that during the processes of derivation they are to be kept constant. The related initial and boundary conditions remains unchanged.

After some mathematical manipulations, according to the discretization procedure underlined above, Eqs. (20) and (4) lead, respectively, to

$$U_i^{j+1} = U_i^j + \frac{\Delta t\, x_i^j v^j}{2\Delta x^j s^j}\left(U_{i+1}^j - U_{i-1}^j\right) + \frac{\Delta t}{(\Delta x^j)^2}\left(U_{i+1}^j - 2U_i^j + U_{i-1}^j\right) + f\left(x_i^j, t_j\right)\Delta t, \quad i = 2, 3, \ldots, N \tag{21}$$

$$v^j = \left(\frac{\mathrm{d}s}{\mathrm{d}t}\right)^j = \frac{4U_N^j - U_{N-1}^j}{2\Delta x^j} \tag{22}$$

A three-term backward approximation is used to evaluate numerically the temperature gradient in the energy balance at the moving boundary. It should be noted that Eq. (22) takes into account the boundary condition (3) ($U_{N+1}^j = 0$, $j = 1, 2, \ldots$) and allows locating the moving boundary at the next time step according to the following approximation:

$$s^{j+1} = s^j + \Delta t v^j \tag{23}$$

Given the time stepping Δt and the number of subdivisions N, the numerical solution procedure starts from known values of s^j and U_i^j ($i = 1, 2, \ldots, N+1$) at time $j\Delta t$ and proceeds as outlined in the following:

(i) evaluate the space step $\Delta x^j = s^j/N$ and the nodal positions $x_i^j = (i-1)\Delta x^j$;
(ii) evaluate the velocity v^j using Eq. (22);
(iii) calculate U_1^{j+1} using discretized form of *FBC* (Eq. (7));
(iv) calculate U_i^{j+1} for $i = 2, 3, \ldots, N$, from Eqs. (21) and set $U_{N+1}^{j+1} = 0$;
(v) calculate s^{j+1} using Eq. (23).

3.2. Boundary immobilization method (BIM)

Introducing the Landau [51] coordinate transformation $\xi = x/s$, Crank [31] developed a method using constant time Δt and space $\Delta\xi$ stepping. In the new coordinate system (ξ, t), the moving front is fixed at $\xi = 1$ and the energy transport equation takes the form

$$\frac{\partial U}{\partial t} = \frac{\xi}{s}\frac{\mathrm{d}s}{\mathrm{d}t}\frac{\partial U}{\partial \xi} + \frac{1}{s^2}\frac{\partial^2 U}{\partial \xi^2} + f(\xi s, t), \quad 0 \prec \xi \prec 1,\ t \succ 0 \tag{24}$$

$$\frac{\mathrm{d}s}{\mathrm{d}t} = -\frac{1}{s}\frac{\partial U}{\partial \xi}\Bigg)_{\xi=1} \tag{25}$$

The computational domain is divided into N grids of equal size $\Delta\xi = 1/N$ such that the freezing front coincides with the $N+1$ grid point at any time $t^j = j\Delta t$ with $j = 1, 2, \ldots$. The position of any grid point is given by $\xi_i = (i-1)\Delta\xi$ ($i = 1, 2, \ldots, N+1$) and its temperature by $U_i^j = U(\xi_i, t^j)$.

Eqs. (24) and (25) and the related initial and boundary conditions are solved with an explicit finite difference scheme. For this purpose, the previous discretization procedure is followed and leads to

$$U_i^{j+1} = U_i^j + v^j \frac{\Delta t \xi_i}{2\Delta\xi s^j}\left(U_{i+1}^j - U_{i-1}^j\right) + \frac{\Delta t}{\Delta\xi^2 s^{j2}}\left(U_{i+1}^j - 2U_i^j + U_{i-1}^j\right) + \Delta t\, f\left(\xi_i s^j, t^j\right), \quad i = 2, 3, \ldots, N \tag{26}$$

$$v^j = \left(\frac{\mathrm{d}s}{\mathrm{d}t}\right)^j = \frac{4U_N^j - U_{N-1}^j}{2s^j\Delta\xi} \tag{27}$$

Also, the location of the moving front is updated using the finite difference form (Eq. (23)).

Given the time step Δt and the number of mesh points $(N+1)$, the numerical solution starts with evaluating the space step $\Delta\xi = 1/N$ and locating the grid points, $\xi_i = (i-1)\Delta\xi$. Then, from known values of s^j and U_i^j ($i = 1, 2, \ldots, N+1$) at time $j\Delta t$ the following outlined procedure applies:

(i) evaluate the velocity v^j using Eq. (27);
(ii) calculate U_1^{j+1} using discretized form of *FBC* (Eq. (7));
(iii) calculate U_i^{j+1} for $i = 2, 3, \ldots, N$, from Eqs. (26) and set $U_{N+1}^{j+1} = 0$;
(iv) calculate s^{j+1} using Eq. (23).

When comparing these two schemes, it is observed that the first one updates, at each time step, the vector components x_i^j ($i = 1, 2, \ldots, N+1$) and the space grid Δx^j while the second evaluates these quantities (ξ_i and $\Delta\xi$) once, at the beginning, and keeps them unchanged during the numerical integration process. Therefore, when looking more closely at both numerical schemes (Eqs. (21), (26)), it is found that the components of x_i^j are calculated explicitly through the product $\xi_i s^j$ and the space step Δx^j is calculated at least $2 \times (N-1)$ times ($2N$ times when the fixed boundary is unknown) at each time step through the product $\Delta\xi s^j$ which appears twice in the RHS of the second scheme (Eqs. (26)). Otherwise, the scheme based on BIM requires more CPU time than that deduced from VSGM even though both schemes lead to the same solution as it will be shown next.

3.3. Resulting numerical scheme (ResNS)

Up to this point, the present section does nothing more than considering with more details the usual analysis [5]. It is worth noticing that both previous numerical schemes are exactly those considered by Kutluay [40] for two Stefan problems

with forcing term. According to the latter work, numerical results, as presented by the author, seem to show that VSGM predicts more accurately both nodal temperatures, freezing front location and velocity than BIM. Let us now analyze the detailed solutions.

First, we note that both methods evaluate, independently, the nodal temperatures and the interface position at time t^{j+1}. Moreover, the interface must be located before considering the next integration step, since the latter occurs explicitly in the discretized diffusion equations (Eqs. (20), (24)). Then, the front is fixed to the last grid point, explicitly in the first method by updating the space step size at each integration and implicitly in the second through the variable transform. That justifies the classification of both techniques as front-fixing methods. Furthermore, it can be seen that both methods, locate the moving front using Eq. (23) where v^j is given by either Eq. (22) or Eq. (27) which, for a given number of mesh points $(N+1)$ and initial interface position (s^j) as well as nodal temperatures $(U_i^j,\ i=1,2,\ldots,N+1)$, lead to the same velocity value. Then, setting $\Delta x^j = s^j/N$ and $\Delta\xi = 1/N$ in these relations, gives

$$v^j = \left(\frac{\mathrm{d}s}{\mathrm{d}t}\right)^j = \frac{N}{2s^j}\left(4U_N^j - U_{N-1}^j\right) \tag{28}$$

For a given initial guess and domain subdivision, both numerical schemes (Eqs. (20), (24)) give the same solution which, by setting $x_i^j = (i-1)s^j/N$ and $\xi_i = (i-1)/N$ in the first and second numerical schemes, reads as follows:

$$\begin{aligned} U_i^{j+1} &= U_i^j + \frac{(i-1)\Delta t}{4}\frac{N}{(s^j)^2}\left(4U_N^j - U_{N-1}^j\right)\left(U_{i+1}^j - U_{i-1}^j\right) \\ &\quad + \frac{N^2\Delta t}{(s^j)^2}\left(U_{i+1}^j - 2U_i^j + U_{i-1}^j\right) + f\left(\frac{i-1}{N}s^j, t^j\right)\Delta t, \quad i = 2,3,\ldots,N \end{aligned} \tag{29}$$

In contradiction with Ref. [40], it appears, as shown, that both resulting schemes lead to an identical computational algorithm and express, therefore, the same solution.

Before introducing some modifications on these schemes and numerical computations, it is worth noting for each problem the finite difference form of the fixed boundary condition (*FBC*). In the case of Problem 1, the condition is of a first kind and can be introduced directly into the algorithms as follows:

$$U_1^{j+1} = 0, \quad j \geqslant 0 \tag{30}$$

For Problem 2, the condition is of a second kind and the usual treatment of this condition introduces a fictive start node. The heat flux at this boundary is replaced by a central difference using both neighbor nodes ($i=0$ and $i=2$) and solve for the fictive node temperature, U_0^j, by applying Eq. (17) to get

$$U_0^j = U_2^j + \frac{2}{N}s^j e^{t^j} \tag{31}$$

Assuming, then, that the finite difference approximations of the diffusion equation is valid on the first node and eliminating U_0^j, using the previous equation, we obtain

$$U_1^{j+1} = U_1^j + 2\frac{N\Delta t}{s^j}\left[\frac{N}{s^j}\left(U_2^j - U_1^j\right) + \mathrm{e}^{t^j}\right] \tag{32}$$

Through this analysis, it is shown that both numerical schemes can be seen as two different expressions of unique solution, having then the same stability, consistency and accuracy. The two formulations differ only in the CPU time required to obtain the solution as outlined in the previous section.

In a recent paper, Yigit [42] studied the solidification of a semi-infinite liquid lying on a finite slab. The author developed a numerical scheme on the basis of the VSGM. The proposed solution updates the nodal temperatures in the solidified layer using a predictor–corrector procedure. The diffusive and convective terms in the heat transport equation (20) are treated separately. The diffusive term will serve to predictions which will be then corrected with the help of the convective term. The latter being replaced by a finite difference approximation expressed at time t^{j+1}, whose truncation error is on the order of 1 with respect to Δx. However, this fact reduces the accuracy of the solution; furthermore, the predictor–corrector procedure increases the CPU time.

3.4. Modified numerical scheme (ModNS)

Considering the boundary immobilization formulation, Kutluay et al. [38] made a change of variable by setting $\sigma = s^2$ in Eqs. (24) and (25). A new numerical scheme is obtained and designated as boundary immobilization method by the authors. Taking into account that the latter can be deduced from the variable space grid formulation (Eqs. (20), (4)), it is referred in the present study as modified numerical scheme (ModNS). Applying then the change of the variable to the finite difference approximation of the Stefan condition (Eq. (28)) to get

$$\left(\frac{\mathrm{d}\sigma}{\mathrm{d}t}\right)^j = N\left(4U_N^j - U_{N-1}^j\right) \tag{33}$$

This equation allows one to update the value of the variable σ throughout the forward finite difference for the LHS term, that is:

$$\sigma^{j+1} = \sigma^j + N\Delta t\left(4U_N^j - U_{N-1}^j\right) \tag{34}$$

The finite difference scheme (Eqs. (29)) becomes

$$U_i^{j+1} = U_i^j + \frac{(i-1)\Delta t}{4\sigma^j}\left(\frac{\mathrm{d}\sigma}{\mathrm{d}t}\right)^j\left(U_{i+1}^j - U_{i-1}^j\right) + \frac{N^2\Delta t}{\sigma^j}\left(U_{i+1}^j - 2U_i^j + U_{i-1}^j\right) + \Delta t f\left(\frac{i-1}{N}\sqrt{\sigma^j}, t^j\right), \quad i = 2, 3, \ldots, N \tag{35}$$

One should note that the procedure evaluating the velocity is not specified in the paper [38]. Once the interface is located at time t^{j+1} from the relation $s^{j+1} = \sqrt{\sigma^{j+1}}$, the velocity can be evaluated using either central, backward or forward finite difference approximations or just deduced from Eq. (33) as considered in the present study

$$v^j = \frac{1}{2\sqrt{\sigma^j}}\left(\frac{\mathrm{d}\sigma}{\mathrm{d}t}\right)^j \tag{36}$$

the numerical scheme is then completed by $U_{N+1}^{j+1} = 0$ and *FBC* which is replaced by Eq. (30) in the case of Problem 1 and by the following for Problem 2

$$U_1^{j+1} = U_1^j + 2\frac{N\Delta t}{\sigma^j}\left[N\left(U_2^j - U_1^j\right) + \sqrt{\sigma^j}e^{t^j}\right] \tag{37}$$

The accuracy of the numerical solutions, of both previous schemes (ResNS and ModNS) when applied to Problem 2, are studied by Kutluay et al. [38]. The authors outlined that the modified numerical scheme is less accurate in predicting the interface movement than the original scheme but is slightly more accurate when determining the temperature distribution.

3.5. Refined numerical scheme (RefNS)

Wood [50] showed that the solution accuracy, obtained using the heat balance integral method, depends largely on the efficient use of the Stefan condition in the analysis. This can be understood since the movement of the phase change front is governed by the latter equation. According to this result, it is proposed to reduce the truncation error of the finite difference formula approximating numerically the temperature gradient in the Stefan condition (4). A fourth-term backward finite difference leads to

$$v^j = \frac{1}{6\Delta x^j}\left(18U_N^j - 9U_{N-1}^j + 2U_{N-2}^j\right) \tag{38}$$

where the boundary condition $U_{N+1}^j = 0$ is accounted for. The numerical scheme obtained using variable space grid formulation is considered since it requires less CPU time as outlined at the end of Section 3.2. Except the above modification expressed by Eq. (38), the refinement procedure does not bring significant changes in the algorithm developed using VSGM.

4. Numerical computations and discussion

This section is devoted to some numerical results related to the movement, i.e. location and velocity, of the freezing front as well as to the nodal temperatures with a particular interest to the fixed boundary in the case of Problem 2. We denote by e_s^j, e_v^j and $e_{U_i}^j$ the relative error at time t^j on position and velocity of the moving front and the temperature of the ith node respectively. These relative errors are defined below and provided to test the accuracy of the three numerical schemes.

$$e_s^j = 10^2\left|\frac{s^j - s(t^j)}{s(t^j)}\right|, \qquad e_v^j = 10^2\left|\frac{v^j - v(t^j)}{v(t^j)}\right|, \qquad e_{U_i}^j = 10^2\left|\frac{U_i^j - U(x_i^j, t^j)}{U(x_i^j, t^j)}\right| \tag{39}$$

$s(t^j)$ and $v(t^j)$ are the exact values of the location and the velocity of the moving boundary at time t^j while s^j and v^j refer to the approximate values obtained using the numerical schemes. $U(x_i^j, t^j)$ and U_i^j are the exact and the approximate numerical values of ith mesh point at this time. The average value of the relative error, $\|e\|^j$, as defined below refers to the weighted 1-norm error in Refs. [38,40].

Table 1
Values of the location and velocity of the moving front as predicted by different numerical schemes and exact solution at time $t = 0.5$ in the case of Problem 1. The time step Δt is considered constant and equal to $e^{2t_0}/(2N^2)$.

Node number, N	Scheme	Numerical solutions				
		Position, s	Error, e_s (%)	Velocity, v	Error, e_v (%)	Average error on U, $\bar{e}_U$
10	ResNS	1.646602	0.128555	1.646731	0.120717	0.004323
	ModNS	1.644863	0.234026	1.645991	0.165610	0.006820
	RefNS	1.646613	0.127853	1.646777	0.117904	0.004309
20	ResNS	1.648193	0.032030	1.648235	0.029488	0.001268
	ModNS	1.647753	0.058722	1.648041	0.041274	0.002066
	RefNS	1.648194	0.031979	1.648238	0.029291	0.001267
40	ResNS	1.648589	0.008000	1.648600	0.007327	0.000367
	ModNS	1.648479	0.014694	1.648551	0.010310	0.000610
	RefNS	1.648589	0.007996	1.648601	0.007314	0.000367
80	ResNS	1.648688	0.001999	1.648691	0.001829	0.000105
	ModNS	1.648661	0.003674	1.648679	0.002577	0.000177
	RefNS	1.648688	0.001999	1.648691	0.001828	0.000105
	Exact values	1.648721	–	1.648721	–	–

Table 2
Values of the location and velocity of the moving front as predicted by different numerical schemes and exact solution at the final time $t = 1$ in the case of Problem 2. The time step Δt is considered constant and equal to $t_0^2/(2N^2)$.

Node number, N	Scheme	Numerical solutions				
		Position, s	Error, e_s (%)	Velocity, v	Error, e_v (%)	Average error on U, $\bar{e}_U$
10	ResNS	0.999047	0.095338	0.997420	0.258021	0.002796
	ModNS	0.999024	0.097585	0.997442	0.255777	0.002854
	RefNS	1.000023	0.002304	1.000366	0.036626	0.000526
20	ResNS	0.999766	0.023356	0.999373	0.062676	0.000843
	ModNS	0.999761	0.023919	0.999379	0.062114	0.000861
	RefNS	0.999997	0.000305	1.000055	0.005494	0.000141
40	ResNS	0.999942	0.005778	0.999846	0.015436	0.000248
	ModNS	0.999941	0.005918	0.999847	0.015296	0.000254
	RefNS	0.999998	0.000180	1.000009	0.000950	0.000039
80	ResNS	0.999963	0.001437	0.999902	0.003830	0.000072
	ModNS	0.999962	0.001472	0.999902	0.003795	0.000073
	RefNS	0.999999	0.000057	1.000006	0.000186	0.000011
	Exact values	1.000000	–	1.000000	–	–

$$\bar{e}_U^j = \frac{1}{M}\sum_{i=m}^{N}\left|\frac{U_i^j - U(x_i^j, t^j)}{U(x_i^j, t^j)}\right| \tag{40}$$

where (m, M) are equal to $(2, N-1)$ and $(1, N)$ for Problem 1 and Problem 2 respectively.

To start numerical calculations for Problem 2, and to circumvent the singularity at time $t = 0$, i.e. $s(t) = 0$ and $U(x, t) = 0$, temperature distribution and the corresponding position of the moving front given by exact solution (Eqs. (18), (19)) are considered at the initial time $t_0 = 0.1$ (used in Ref. [38]). Whereas, numerical schemes applied to Problem 1, are self-starting by using the given initial conditions (Eqs. (12), (13)) to initialize numerical procedure. The schemes are based on explicit finite difference approximation restricting then the choice of the time step due to stability consideration. According to Kutluay et al. [38], the use of the von Neumann analysis limits the lower value of the time step to $(s^j)^2/(2N^2)$. The problems considered in the present study are both continuous such that the thickness of the formed layer increases without bound $s^j > s_0$ (for $j = 1, 2, \ldots$). Consequently and by virtue of the initial conditions (Eqs. (13), (19)), the time step size $\Delta t = s_0^2/(2N^2)$ is considered corresponding then to $\Delta t = t_0^2/(2N^2)$ and $\Delta t = 1/(2N^2)$ for Problem 1 and Problem 2, respectively.

First of all, exact solutions of Problem 1 and Problem 2 are used to study the effects of the number of mesh points on the solution accuracy. Tables 1 and 2 summarize some numerical results concerning the predicted position and velocity of the moving boundary for Problem 1 and Problem 2 at time $t = 0.5$ and $t = 1$ respectively. The corresponding percentage relative errors as well as the average relative error on the nodal temperatures are included in those tables. The schemes, presented in Sections 3.3, 3.4 and 3.5, were tested for four values of step size, $N = 10, 20, 40$ and 80.

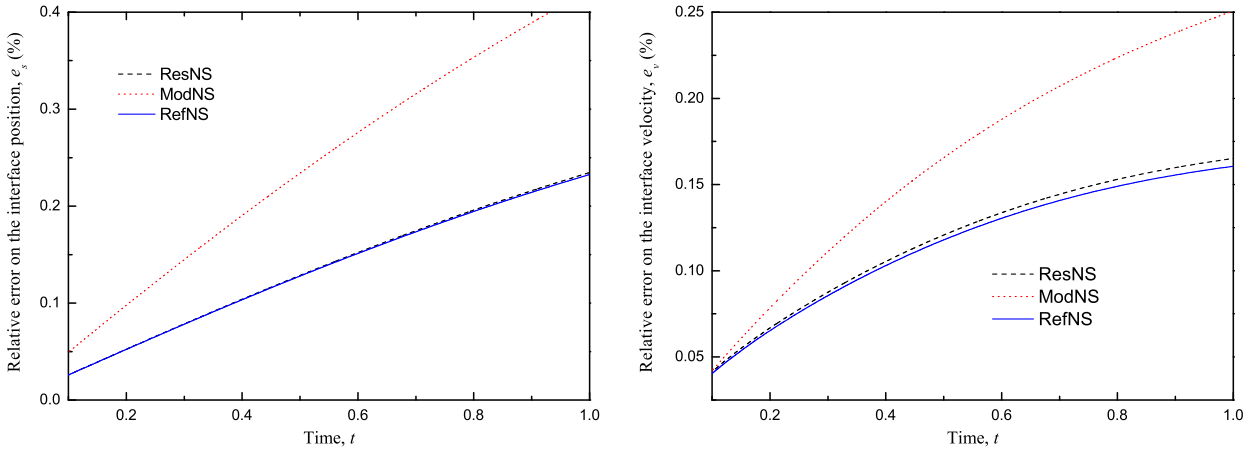

Fig. 1. Relative error on the predicted position and velocity of the moving boundary for $N = 10$ in the case of Problem 1.

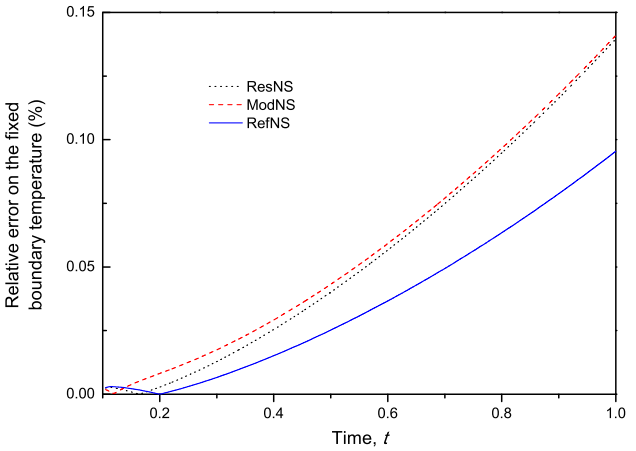

Fig. 2. Relative error on the predicted fixed boundary temperature for $N = 10$ in the case of Problem 2.

It should be noticed that the expected convergence of the solutions with the reduction of the space step size is demonstrated. Furthermore, the three schemes show a very appreciable precision in particular for Problem 1 taking into account that the error is on the same order. However, in the case of Problem 2 the solution using the refined numerical scheme (RefNS) exhibits noticeably less error that the two others (ResNS and ModNS). As a matter of fact, the latter schemes have a similar error while the new scheme has a definite improvement in the precision. It should be observed that all three schemes underestimate the interface position. Nonetheless the error associated to the second scheme (ModNS) is higher than the two others. This is expected since the interface position increases continuously making s^{j+1} always greater than s^j that is: $s^{j+1} + s^j > 2s^j$. Eq. (34) can be seen as a linearized form of the following

$$s^{j+1} = s^j + \frac{N\Delta t}{s^{j+1} + s^j}\left(4U_N^j - U_{N-1}^j\right)$$

It is now interesting to examine the evolution of these relative errors with respect to time. For that purpose, N was chosen as 10 and the relative errors are depicted in Figs. 1–4. Fig. 1 shows the relative error on the predicted position and velocity of the moving boundary in the case of Problem 1. In the ModNS the error is nearly the double of the two others for both the position and the velocity. One should observe that the lowest error is provided by the refined numerical scheme. Fig. 2 depicts the relative error on the exchange surface temperature ($x = 0$) as function of time predicted by the schemes discussed. The refined numerical scheme gives better results than the two others which show a comparable accuracy. On the overall, the relative error does not exceed 0.15%. On the other hand Fig. 4 shows a definite improvement of RefNS. As a matter of fact the average value of the relative errors computed from N-node temperatures, as show in Fig. 4, is less than 0.05%. Fig. 3 examines the case of Problem 2. The relative errors of the interface position and velocity are on the same order for the ResNS and the ModNS. On the other hand the gap between the RefNS and the two other methods is very large, showing then the accuracy of the RefNS. By comparing the ModNS and the ResNS, one could notice that the ResNS is less accurate with respect to the evaluation of the interface position while the velocity determination exhibits a higher accuracy. This seems, a priori, in contradiction. However, this is explained by the fact that the starting computation in the

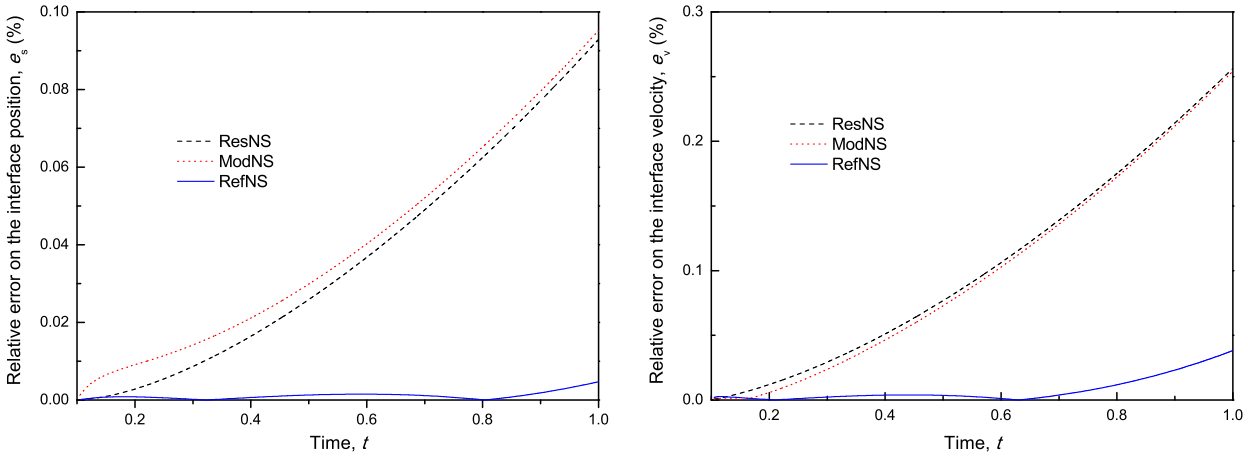

Fig. 3. Relative error on the predicted position and velocity of the moving boundary for $N = 10$ in the case of Problem 2.

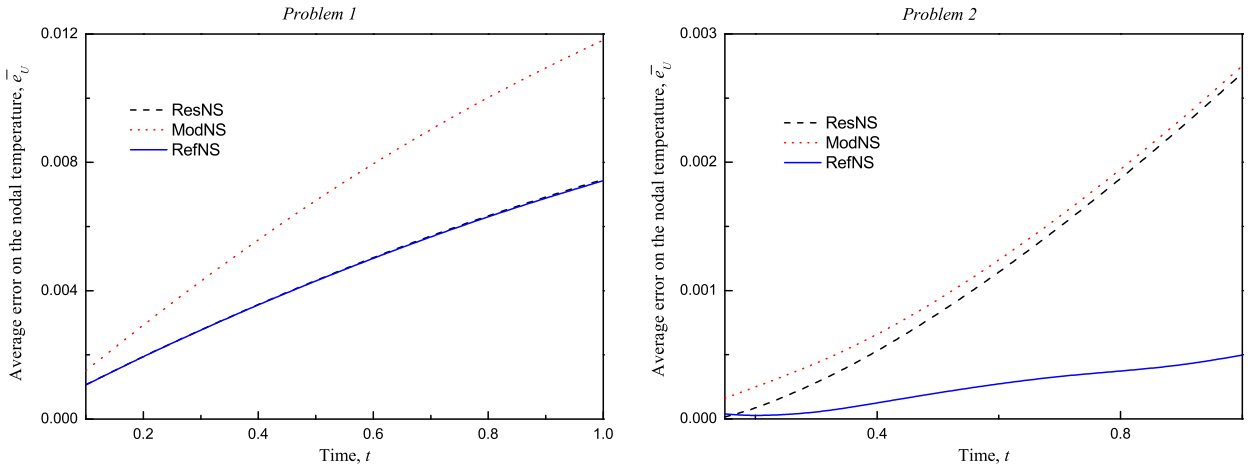

Fig. 4. Average relative error on the predicted nodal temperature for $N = 10$.

ModNS is not precise that is: the error associated to the interface location is very high. One should observe that, on the overall, the error increases with time as depicted in all figures. This is expected since the truncation error is space step dependent which in turns increases. Finally it is worth noting that in all cases the RefNS gives better results.

5. Conclusion

In this article three numerical schemes, based on variable space grid or boundary immobilization methods, were applied to the two Stefan problems. It was shown that the numerical schemes obtained by the above cited methods lead to a unique solution. However, it should be observed that the boundary immobilization method requires more computational time than the variable space grid approach. The modified numerical scheme proposed by Kutluay et al. [38] was considered but does not bring any additional refinements. On the overall the three numerical schemes solved the models considered quite satisfactorily. The numerical results show that the use of the four-term backward finite difference approximation to evaluate the heat flux at the moving boundary refines the solution accuracy without affecting the central processing time.

Acknowledgements

The authors gratefully acknowledge financial support from the M.E.S.R.S. (Ministère de l'enseignement supérieur et de la recherche scientifique, Algeria) and Université de Nantes: GEPEA (Génie des procédés. Environnement. Agroalimentaire). The work was also supported by the ESA (European Space Agency) and BELSPO (Belgian Science Policy) PRODEX programme. P.C. gratefully acknowledges financial support of the Fonds de la Recherche Scientifique – F.N.R.S. (Belgium).

References

[1] H.S. Carslaw, J.C. Jaeger, Conduction of Heat in Solids, second ed., Oxford University Press, 1959.
[2] L. Junyi, X. Mingyu, Some exact solutions to Stefan problems with fractional differential equations, J. Math. Anal. Appl. 351 (2009) 536–542.
[3] V. Voller, An exact solution of a limit case Stefan problem governed by a fractional diffusion equation, Int. J. Heat Mass Transfer 53 (2010) 5622–5625.
[4] R.S. Gupta, Some numerical and integral methods for solving moving boundary problems in heat flow and diffusion, Ph.D. thesis, Brunel University, Uxbridge, 1972.
[5] J. Crank, Free and Moving Boundary Problems, Clarendon Press, Oxford, 1984.
[6] J.M. Hill, One-Dimensional Stefan Problems: An Introduction, Longman Scientific and Technical, New York, USA, 1987.
[7] V. Alexiades, A.D. Solomon, Mathematical Modelling of Melting and Freezing Processes, Hemisphere Publishing Corporation, USA, 1993.
[8] L.S. Yao, J. Prusa, Melting and freezing, Adv. Heat Transfer 19 (1989) 1–95.
[9] R.M. Furzeland, A comparative study of numerical methods for moving boundary problems, J. Inst. Math. Appl. 5 (1980) 411–429.
[10] M. El Ganaoui, P. Bontoux, An homogenization method for solid–liquid phase change during directional solidification, in: R.A. Nelson, T. Chopin, S.T. Thynell (Eds.), Numerical and Experimental Methods in Heat Transfer, vol. 361, ASME, H.T.D., 1998, pp. 453–469.
[11] M. El Ganaoui, P. Bontoux, A. Lamazouade, E. Leonardi, G. De Vahl Davis, Computational model for solutal convection during directional solidification, Numer. Heat Transfer Part B 41 (2001) 325–338.
[12] E.A. Semma, M. El Ganaoui, R. Bennacer, Lattice Boltzmann method for melting/solidification problems, C. R. Mecanique 335 (2007) 295–303.
[13] Z. Yang, M. Sen, S. Paolucci, Solidification in finite slab with convective cooling and shrinkage, Appl. Math. Model. 27 (2003) 733–762.
[14] J. Caldwell, Y.Y. Kwan, On the perturbation method for the Stefan problem with time-dependent boundary conditions, Int. J. Heat Mass Transfer 46 (2003) 1497–1501.
[15] T.R. Goodman, The heat-balance integral and its application to problems involving a change of phase, Trans. ASME 80 (1958) 335–345.
[16] N. Sadoun, E.K. Si-Ahmed, P. Colinet, J. Legrand, On the Goodman heat balance integral method for Stefan-like problems: Further considerations and refinements, Thermal Sci. 13 (2) (2009) 81–96.
[17] A.P. Roday, M.J. Kazmierczak, Analysis of phase-change in finite slabs subjected to convective boundary conditions: Part I – Melting, Int. Rev. Chem. Eng. 1 (2009) 87–99.
[18] A.P. Roday, M.J. Kazmierczak, Analysis of phase-change in finite slabs subjected to convective boundary conditions: Part II – Freezing, Int. Rev. Chem. Eng. 1 (2009) 100–108.
[19] N. Sadoun, E.K. Si-Ahmed, A new analytical expression of the freezing constant in the Stefan problem with initial superheat, Numer. Meth. Therm. Probl. 9 (1995) 843–854.
[20] N. Sadoun, E.K. Si-Ahmed, P. Colinet, On the refined integral method for the one-phase Stefan problem with time-dependent boundary conditions, Appl. Math. Model. 30 (2006) 531–544.
[21] T.G. Myers, Optimal exponent heat balance and refined integral methods applied to Stefan problems, Int. J. Heat Mass Transfer 53 (2010) 1119–2010.
[22] N. Sadoun, E.K. Si-Ahmed, P. Colinet, New analytical expression for the freezing constant using the refined integral method with cubic approximant, in: MULTIFLOW Conference 2010, Brussels, November 8–10, 2010.
[23] B. Sudhakar, An integral method for non-linear moving boundary problems, Chem. Eng. Sci. 47 (1992) 475–479.
[24] B. Sudhakar, On integral iterative formulation in classical Stefan problem, Chem. Eng. Sci. 47 (1992) 3158–3162.
[25] J. Hristov, Heat balance integral to fractional (half-time) heat diffusion sub-model, Thermal Sci. 14 (2010) 291–316.
[26] S.R. Coriell, G.B. McFadden, R.F. Sekerka, W.J. Boettinger, Multiple similarity for solidification and melting, J. Cryst. Growth 191 (1998) 573–585.
[27] V.M. Barragan, J.M. Arias, M. Dominguez, C. Garcia, Testing the computer assisted solution of the electrical analogy in a heat transfer process with a phase change which has an analytical solution, Int. J. Refrig. 24 (2001) 532–537.
[28] V. Voller, M. Cross, Accurate solutions of moving boundary problems using the enthalpy method, Int. J. Heat Mass Transfer 24 (1981) 545–556.
[29] V.R. Voller, C.R. Swaminathan, B.G. Thomas, Fixed grid techniques for phase-change problems: A review, Int. J. Numer. Eng. 30 (1990) 857–898.
[30] A.A. Samarski, P.N. Vabishchevich, O.P. Iliev, A.G. Churbano, Numerical simulation of convection/diffusion phase change problems: A review, Int. J. Heat Mass Transfer 36 (1993) 4095–4106.
[31] J. Crank, Two methods for the solution of moving boundary problems in diffusion and heat flow, Quart. J. Mech. Appl. Math. 10 (1957) 202–231.
[32] W.D. Murray, F. Landis, Numerical and machine solutions of the transient heat conduction problems involving melting or freezing, J. Heat Transfer (C) 81 (1959) 106–112.
[33] A.K. Verma, S. Chandra, B.K. Dhindaw, An alternative fixed grid method for solution of the classical one-phase change Stefan problem, Appl. Math. Comput. 158 (2004) 573–584.
[34] J. Douglas, T.M. Callie, On the numerical integration of a parabolic differential equation subject to a moving boundary condition, AFS Cast Metals Res. 10 (1974) 26–29.
[35] J.S. Goodling, M.S. Khader, Inward solidification with a convective boundary condition, ASME J. Heat Transfer 96 (1974) 114–115.
[36] R.S. Gupta, D. Kumar, A modified variable time-step method for the one-dimensional Stefan problem, Comput. Meth. Appl. Mech. Eng. 23 (1980) 101–108.
[37] N. Sadoun, E.K. Si-Ahmed, J. Legrand, On heat conduction with phase change: accurate explicit numerical method, J. Appl. Fluid Mech. 5 (2012) 105–112.
[38] S. Kutluay, A.R. Bahadir, A. Ozdeş, The numerical solution of one-phase classical Stefan problem, J. Comput. Appl. Math. 81 (1997) 135–144.
[39] S. Savoviç, J. Caldwell, Finite difference solution of one-dimensional Stefan problem with periodic boundary conditions, Int. J. Heat Mass Transfer 46 (15) (2003) 2911–2916.
[40] S. Kutluay, Numerical schemes for one-dimensional Stefan-like problems with a forcing term, Appl. Math. Comput. 168 (2005) 1159–1168.
[41] S. Savoviç, J. Caldwell, Numerical solution of Stefan problem with time-dependent boundary conditions by variable space grid method, Thermal Sci. 13 (4) (2009) 165–174.
[42] F. Yigit, One-dimensional solidification of pure materials with a time periodically oscillating temperature boundary condition, Appl. Math. Comput. 217 (2011) 6541–6555.
[43] R.C. Dix, J. Cizek, The isotherm migration method for transient heat conduction analysis, in: Proc. Fourth Int. Heat Trans. Conf., vol. 1, Paris, 1970.
[44] F.L. Chernousko, Solution of non-linear heat conduction problems in media with phase changes, Int. Chem. Eng. 10 (1970) 42–48.
[45] J. Crank, T. Ozis, Numerical solution of free boundary problem by interchanging dependent and independent variables, J. Inst. Math. Appl. 26 (1980) 77–85.
[46] A.S. Wood, A note on the use of isotherm migration method, J. Comput. Appl. Math. 36 (1991) 133–147.
[47] S. Kutluay, A. Esen, An isotherm migration formulation for one-phase Stefan problem with a time dependent Neumann condition, Appl. Math. Comput. 150 (2004) 59–67.
[48] A. Fasano, M. Primicerio, Free boundary problems for nonlinear parabolic equations with nonlinear free boundary conditions, J. Math. Anal. Appl. 72 (1979) 247–273.
[49] K.H. Hoffmann (Ed.), Freie Randwert probleme I, II, III, Preprint Nos. 22, 28, 34, Fachbereich Mathematik, Freie Univ. Berlin, Berlin, 1977.
[50] A.S. Wood, A new look at the heat balance integral method, Appl. Math. Model. 25 (10) (2001) 815–824.
[51] H.G. Landau, Conduction of heat in solid, Quart. J. Mech. Appl. Math. 8 (1950) 81–94.